Optimal Demand Response for Distribution Feeders with Existing Smart Loads

Abolfazl Mosaddegh, *Student Member, IEEE,* Claudio A. Cañizares, *Fellow, IEEE,* and Kankar Bhattacharya, *Fellow, IEEE*

***Abstract*—Load characteristics play an important role in distribution systems, which are traditionally designed to supply peak load; hence, decreasing this peak can considerably reduce overall grid costs. Basic components of smart grids such as smart meters allow two-way communication between the utilities and customers; in this context, controllable smart loads are being introduced, which allow developing and implementing Energy Management Systems (EMSs) for customers and distribution feeders. Therefore, this paper studies the impact of existing smart loads, in particular Peaksaver PLUS™ (PS+) loads in Ontario, Canada, to reduce summer peak loads for distribution feeders. A Neural Network (NN) model of controllable loads is developed and integrated into an unbalanced Distribution Optimal Power Flow (DOPF) model to optimally control tap changers and switched capacitors, as well as sent signals to programmable thermostats of air conditioners in residential buildings, in particular those associated with the PS+ program. The developed integrated DOPF is tested and validated using a practical system, demonstrating the benefits of using existing controllable loads to optimally operate distribution feeders.**

***Keywords*—Demand response, distribution system optimal power flow, energy management system, load modeling, neural networks, real-time application, smart grid.**

NOMENCLATURE

Indices

c, n	Nodes, $c, n = 1, ..., N_N$.
fc	Per-phase controllable tap changers.
h	Time interval, $h = 1, ..., 24$.
lf	Substation feeder.
p	Phases, $p = a, b, c$.
r_n	Receiving-ends connected at node n.
s_f	Substation node.
s_n	Sending-ends connected at node n.

Parameters

$C^{max}_{p,n}$	Total number of capacitor blocks available in capacitor banks.
$\overline{I}_{lf}$	Maximum feeder current limit [A].
N_N	Total number of nodes.
P_{cons}	Target active power demand [kW].
P_{lim}	Active power demand limit [kW].
$P^g_{p,n,h}$	Generated active power [kW].
$Q^g_{p,n,h}$	Generated reactive power [kVar].
$T^{max}_{p,n}$	Maximum hours of Programmable Communication Thermostat (PCT) operation [h].
$\overline{TAP}_{p,fc}$	Maximum tap changer position.
$\underline{TAP}_{p,fc}$	Minimum tap changer position.
$\overline{V}$	Maximum voltage limit [kV].
$\underline{V}$	Minimum voltage limit [kV].
$Y_{p,nc,h}$	Nodal admittance matrices of the power system from node n to node c [μS].
β	Peak load penalty factor.
θ_h	Ambient temperature [°C].
σ_h	Time of Use (TOU) tariff [\$/kWh].

Variables

$cap_{p,n,h}$	Number of capacitor blocks switched on.
E_{loss}	Energy loss [kWh].
$I_{lf,p,h}$	Feeder current phasor [A].
$I_{p,n,h}$	Current injection phasor [A].
J	Objective function.
$P_{feeder_{p,h}}$	Substation feeder active power [kW].
$Psl_{p,n,h}$	Simulated active power demand for controllable loads [kW].
$tap_{p,fc,h}$	Tap position.
$V_{p,n,h}$	Voltage phasor [kV].
$\mu_{p,n,h}$	Binary ON/OFF signal (0 for no change in PCT setpoint, and 1 for PCT setpoint increased by 2°C).

I. INTRODUCTION

Monitoring and control of distribution systems are integral aspects of smart grids, carried out based on various objectives/programs at the feeder level such as Voltage/Var Control (VVC), Demand Response (DR), Distribution Management Systems (DMSs), system reconfiguration, and system restoration [1]–[3]. Furthermore, at the customer end, real-time monitoring and control, associated with Energy Management Systems (EMSs) at residential, industrial, commercial, or agricultural sites, are also important features of smart grids [4], [5]. Controllable loads are being integrated into Distribution System Automation (DSA) techniques and tools to affect load profiles, which benefits both customers and Local Distribution Companies (LDCs). While reducing energy consumption and costs are of interest to customers, reducing the peak load and reshaping load profiles, which increase system sustainability, are mainly of interest to LDCs [4], [6]. Hence, studying the behaviour of controllable loads, their impact on the aggregated load profiles, and their integration in optimal distribution system operation is relevant and timely.

This work was supported by Hydro One Networks, Energent Inc., Milton Hydro Distribution, the Ontario Power Authority (OPA), and the Ontario Centres of Excellence (OCE) under the Energy Hub Management System (EHMS) project (http://www.energyhub.uwaterloo.ca/) and Natural Sciences and Engineering Research Council (NSERC) Smart Microgrid Research Network (NSMG-Net).

A. Mosaddegh, C. A. Cañizares, and K. Bhattacharya ({amosaddegh, ccanizares, kankar}@uwaterloo.ca) are with University of Waterloo, Waterloo, ON, Canada.

DR programs have been introduced so that customers can control and alter their energy consumption, with benefits accruing to both customers and LDCs. Many DR programs are based on the relationship between electricity price and demand, and direct control of customers' loads is one of the realizations of DR programs [7]. Remote systems based on Power Line Carriers (PLCs), internet, and radio wave systems make end-users' devices controllable within a distribution system. Among these controllable devices, monitoring, supervising, and controlling of Heating, Ventilation, and Air Conditioning (HVAC) systems in various facilities have been discussed in the literature [8]–[11]. In particular, the Peaksaver PLUS™ (PS+) program in Ontario, Canada, is a voluntary program to reduce Air Conditioner (AC) demand in the residential and small commercial sector [12]. In this program, smart thermostats, referred to as Programmable Communicating Thermostats (PCTs), are installed to slightly increase the AC temperature setpoints during summer days. Since the contribution of AC, which is about 50% of residential loads, to peak loads is significant, it is estimated in [13] that direct control of AC usage may conserve about 37% of the energy, resulting in savings of $688 million in energy conservation over a 20 year period in Ontario, Canada.

Because of the complexity of controllable loads and insufficient data, it is difficult to use fundamental physical laws for modeling these loads. However, having an accurate model of the customer load profiles is necessary for integrating the loads in distribution system EMS; for this reason, black-box or empirical load models can be used. In such models, a relationship between inputs and outputs is obtained and represented using mathematical equations [14], [15], or by Evolutionary Algorithms (EAs) such as Neural Network (NN) [6], [16], Particle Swarm Optimization (PSO) [17], or Genetic Algorithms (GAs) [18]. In the present work, an NN is used to accurately model controllable loads, while considering the effect of external parameters such as temperature, Time of Use (TOU) tariff, and LDC control signals.

This paper studies the impact and use of existing controllable loads in reducing the peak load in a three-phase unbalanced distribution system. An NN model of controllable PS+ loads is developed and integrated into a Distribution Optimal Power Flow (DOPF) model to optimally control Load Tap Changers (LTCs) and Switched Capacitors (SCs), and send ON/OFF signals to PCTs. Simulation results on a real test feeder demonstrate the effectiveness of the proposed approach. Also, in order to reduce the computational burden of the DOPF model, which is solved using a GA-based technique, and thus making it suitable for real-time applications, a distributed computing approach, based on a Smart Grid Communication Middleware (SGCM) system [19], is used. Hence, the main objectives and contributions of the present work are the following:

- A novel methodology is proposed to generate realistic datasets for home loads including PS+ loads, using the Smart Residential Load Simulator (SRLS) MATLAB® toolbox [20], considering limited availability of field measurements.
- An NN-based model of existing controllable PS+ loads is proposed and developed using the generated load profiles from the SRLS MATLAB® toolbox output.
- An enhanced DOPF model, which considers both VVC and DR objectives, is proposed and developed for an unbalanced distribution feeder that includes existing controllable PS+ loads, to obtain optimal switching decisions for LTCs and SCs, and the ON/OFF signals required for the controllable PS+ loads.
- The impact of the proposed optimal DR is studied and compared to an existing DR program using a realistic distribution feeder, to demonstrate the benefits for distribution systems of the proposed novel approach for various practical operating objectives and scenarios.

The rest of the paper is organized as follows: Section II presents the relevant background, including a brief discussion of DOPF and smart loads. Section III discusses the modeling of controllable smart loads using an NN technique, and demonstrates its application to the existing controllable PS+ loads; the integration of the proposed NN-based PS+ load model into the DOPF is also discussed in this section, together with the GA and distributed computing approaches to solve it. In Section IV, the results of applying the proposed DOPF model to a practical distribution feeder for different scenarios are discussed, and the effect of optimal management of PS+ loads is presented. The main conclusions and contributions of the presented work are highlighted in Section V.

II. Background Review

A. Distribution Optimal Power Flow

Voltage and reactive power control in distribution systems has traditionally been performed by LTCs, SCs, fixed capacitors, and step-voltage regulators. LTCs and step-voltage regulators are voltage-control devices, while SCs and fixed capacitors can regulate both voltage and reactive power; these local controllers have no significant effect on system loading. Since peak loads can be up to 2-3 times the average load, and up to 10 times the minimum load, to properly manage such load variations, centralized control techniques for VVC have been proposed in the literature to maintain voltages within an acceptable range and to minimize energy losses. In the traditional VVC problem, loss minimization is a commonly used objective, as it reduces the reactive power flow in the system by appropriately controlling the node voltages [2]; hence, in this study, minimization of energy losses is considered as a DOPF objective function from a utility perspective. Furthermore, load management associated with DR programs can be integrated with VVC to control and alter the customers' energy consumption in order to obtain benefits such as incentives or lower-priced electricity, with different objectives to satisfy the specific needs of the system. In the present work, the same objective, which is used in the VVC problem, is effectively recast as a DR problem, which is a novel contribution of this paper.

The four major objectives in DR programs depicted in Fig. 1, are peak clipping, valley filling, load shifting, and flexible load shaping [21]. In peak clipping DR programs, the usage during the peak loads is decreased; in valley filling, customers

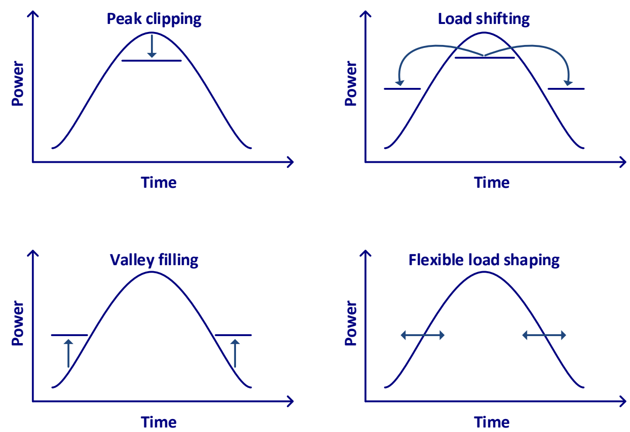

Fig. 1. Major objectives in DR programs [21].

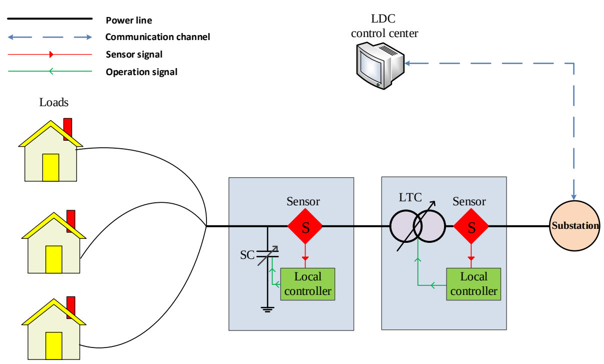

Fig. 2. A conventional distribution system with local controllers for LTCs and SCs [22].

are encouraged to use their equipment during off-peak hours; in load shifting, the electricity usage is shifted from the peak load hours to off-peak hours; and in flexible load shaping, the electricity usage during different times is redistributed. This paper focuses on utility equipment controls, such as LTCs and SCs in the context of peak-clipping DR programs. Thus, models of controllable smart loads are integrated into a DOPF model in order to minimize energy losses as well as reducing peak loads.

The decision variables of the DOPF model described in [19], which is discussed in more detail in Section III, are the optimal set of LTC tap positions, the number of capacitor blocks switched on, and the signals for controllable smart loads. The DOPF solution yields the optimal control signals for LTCs, SCs, and controllable smart loads, i.e., the ON/OFF signal schedule for the PS+ loads.

B. Smart Loads

Traditional VVC in conventional distribution systems is carried out by local controllers with LTCs and SCs, as shown in Fig. 2; lack of two-way communication devices, central controllers, and wide-area measurements have been some of the limitations of these systems [22]. Improvements in

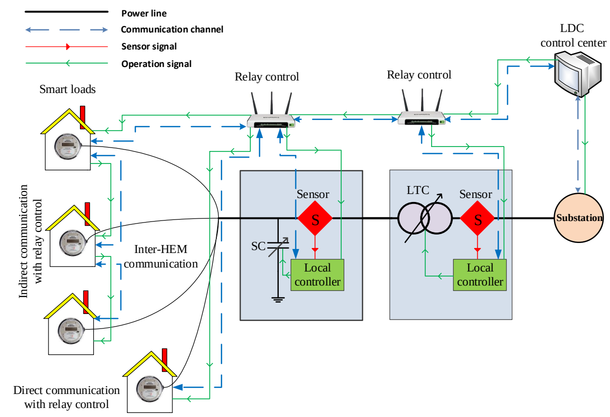

Fig. 3. A typical distribution system with evolving communication and control infrastructure [2].

communication, control, and measurement technologies are transforming these conventional distribution systems into what is now called the smart grid. An important part of these smart grids are smart loads, which include Home Automation Systems (HASs) and Home Energy Management (HEM) systems [4], [23], [24]. Automatic and remote controller switches for lights, setpoints for thermostats, window covers, and other various electrical systems and apparatus are among the features of these systems. Figure 3 presents a typical smart distribution system, depicting the improvements in communication and control infrastructure. A central controller collects load data internally from switches, thermostat setpoints, sensors, measurement devices, and plug-in modules such as audio/video systems and security systems, and collects external data such as weather and energy cost, which may be received fully or partially along with other measurements by the LDC through the Advanced Metering Infrastructure (AMI). In the AMI, a number of neighbors communicate with the LDC through their smart meters, in a so-called Neighborhood Area Network (NAN), and send their data to the utility's Wide Area Network (WAN) [25].

In this study, an NN algorithm is used to model smart loads. The NN model is a function approximation tool, which uses external data to estimate the NN parameters. The system is considered as a black-box, which tries to find the best fitted NN parameters that match the outputs with the targets; for this purpose, the NN should be trained to capture the relationship between the input data and related target data. With a feedback loop control, the output of the NN is compared with the target (i.e., the desired output), and the weights and biases are adjusted between neurons to reduce the error. Depending on the complexity of the system, the number of hidden and output layers of the NN may vary. In this paper, a general NN model of controllable smart loads based on field data is presented next, together with the process of obtaining the model for existing PS+ controllable loads.

III. Mathematical Model

A. Controllable Smart Load

Load modeling plays an important role in power systems. Although there are various measurement devices on the transmission side, unmetered customers on the distribution side have been an issue for DSA. Static load models have been used for various studies in distribution systems [26]. Traditionally, constant impedance or constant power load models have been commonly used [27], which are included in constant impedance (Z), current (I), and power (P) or ZIP load models [19], [28]–[32]. A ZIP load model considers the variation of load with the bus voltage, and its parameters can be fitted to accurately describe the steady-state behaviour of different kinds of loads. Other kind of static load models such as exponential models have also been used [28]. These static models are adequate for steady-state analyses, and hence have been used in DOPF models.

Smart loads include various appliances controlled through an EMS, smart meters, and two-way communication connections among appliances, the LDC, and/or external sources (e.g., weather stations and energy price) [4]. Since customer behaviour may vary by location, preferences, and time of usage, information on customer preferences and the activity level of their appliances are important. However, the only measurement available to LDCs from most residential houses is the energy consumption data derived from their smart meters. These measurements vary widely across households; however, as the load profiles are aggregated, the load profile is smoother, with less variations, thus allowing to better model the load at the feeder level. In order to reduce the peak load at the feeder level, it is assumed in this work that the LDC sends a peak demand cap or temperature setpoint signal to HVACs to modify the load profiles and reduce the customers' peak demand, as in the case of the PS+ program.

In this paper, in order to study the effect of controllable smart loads in residential houses, energy consumption of different houses with realistic data of all appliances, for all days of July 2013, has been modeled in the SRLS [20], which is a MATLAB®-based toolbox developed to model and study electric and thermal loads and sources in residential houses. Smart thermostats, ACs, furnaces, stoves, washers and dryers, refrigerators, wind turbines, solar Photo-Voltaic (PV), and batteries are mathematically modeled in the SRLS to characterize and model residential loads. The consumption and generation profile of each appliance and energy source can be obtained in the SRLS [20], together with the cost of energy supply, at different times, based on user-defined inputs. As shown in Fig. 4, the residential load dataset from each house including the characteristics and time of use of each appliance is modeled in the SRLS, and the obtained load profiles from a group of houses are then aggregated to obtain an average model of the load at a phase and node, which is used to train the NN model that is integrated into the proposed DOPF. Since the focus of this study is at the feeder level, considering an average load model keeps the computational burden of the DOPF model reasonable. The aggregated load of the feeder is obtained by summing the load profiles of the group of houses served by the feeder, with the load profiles of each house being obtained from the SRLS, and the average load is this aggregated load divided by the number of houses served by the feeder.

As a case study, existing PS+ controllable loads are studied. Thus, using an NN, the following residential load profile ($Psl_{p,n,h}$) is estimated as a function of time (h), TOU tariff (σ_h), ambient temperature (θ_h), and binary ON/OFF signals ($\mu_{p,n,h}$) for PCT setpoints of ACs:

$$Psl_{p,n,h} = f(h, \sigma_h, \theta_h, \mu_{p,n,h}) \tag{1}$$

Where, if the PCT setpoint signal is ON ($\mu = 1$), the PCT setpoints are increased by 2°C for a limited time within a day, which decreases the run-cycle of ACs. Therefore, decreasing the demand in all participating residential houses in the PS+ program can lead to a considerable reduction in peak load at the feeder level.

In this paper, after modeling the energy usage of different residential appliances and devices of each house in the SRLS, the aggregated load profiles were obtained. Using the NN MATLAB® toolbox, the aggregated load profile was used for training purposes, obtaining the best fitted NN with one hidden layer with 8 neurons, and one output layer with one neuron, using a Bayesian regularization back-propagation training algorithm. The maximum allowable number of epochs was set to 1000, and the desired gradient to 10^{-7}; 70% of the load dataset was used for training, 15% for validation, and 15% for testing. The Mean Squared Error (MSE) function was used to check the performance of the NN model, and the input data was randomly divided for training, validation, and testing. The NN output yielded an overall R-squared value of 0.9206 and an MSE value of 0.2392 kW^2. Figure 5 presents a comparison of the developed NN output and target for the aggregated loads in July 2013. The peak demand MSE is 0.1860 kW^2, which shows the effectiveness of the obtained NN model.

B. DOPF Model

The general form of a DOPF model with controllable loads can be defined as follows:

$$\begin{aligned}
&\min \;\; J = \text{ Objective function} && \text{(2a)}\\
&\text{s.t.} \;\; \text{Operational and system constraints} && \text{(2b)}\\
&\qquad\;\; \text{Smart load model and constraints} && \text{(2c)}
\end{aligned}$$

Various objective functions such as minimization of energy loss, minimization of energy drawn from the substation, or minimization of energy cost can be adopted in (2a). Operating constraints in (2b) include the power flow equations, as well as bus voltage limits, feeder current limits, and LTC and SC operating limits, as follows:

$$P^g_{p,n,h} - P_{p,n,h} = Re\{V_{p,n,h} I^*_{p,n,h}\} \qquad \forall\, p, n, h \tag{3a}$$

$$Q^g_{p,n,h} - Q_{p,n,h} = Im\{V_{p,n,h} I^*_{p,n,h}\} \qquad \forall\, p, n, h \tag{3b}$$

$$\underline{V} \leq |V_{p,n,h}| \leq \overline{V} \qquad \forall\, p, n, h \tag{3c}$$

$$|I_{lf,p,h}| \leq \overline{I}_{lf} \qquad \forall\, p, h \tag{3d}$$

$$\underline{TAP}_{p,fc} \leq tap_{p,fc,h} \leq \overline{TAP}_{p,fc} \qquad \forall\, p, fc, h \tag{3e}$$

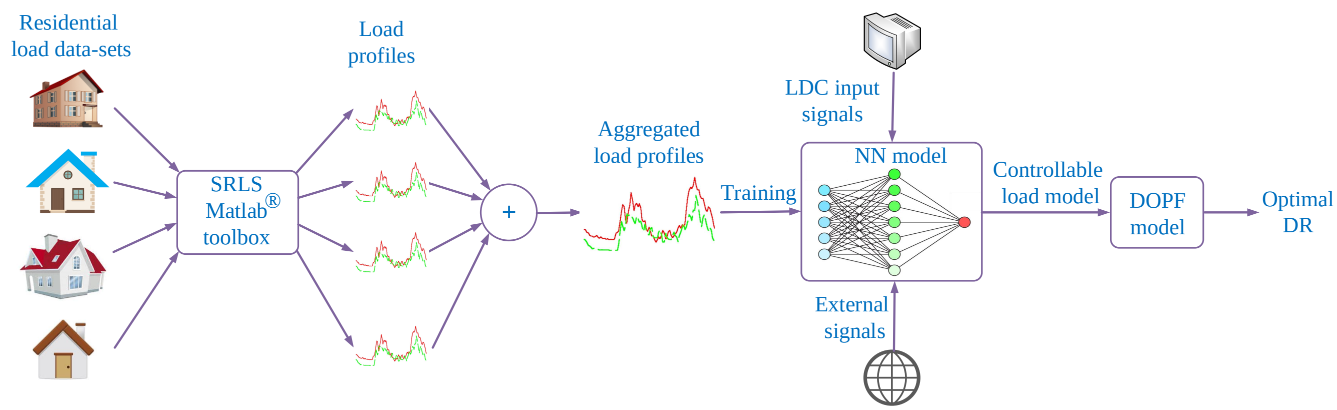

Fig. 4. Schematic of modeling of controllable smart load and its integration into the DOPF model.

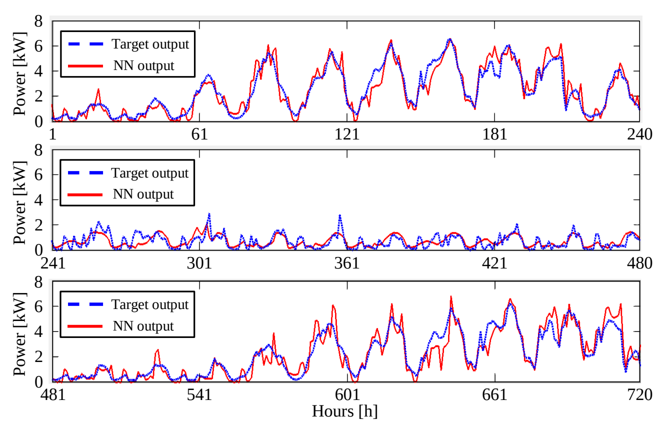

Fig. 5. Comparison of NN output and target for the aggregated loads for 30 days in July 2013.

$$0 \leq cap_{p,n,h} \leq C_{p,n}^{max} \qquad \forall\, p, n, h \tag{3f}$$

where $I_{p,n,h}$ in (3a) and (3b) is defined as:

$$I_{p,n,h} = \sum_{c=1}^{N_N} Y_{p,nc,h} V_{p,c,h} \qquad \forall\, p, n, h \tag{4}$$

Equations (3a) and (3b) correspond to the active and reactive power flow equations; (3c) represents the nodal voltage operating limits; (3d) corresponds to the feeder current operating limits; and (3e) and (3f) represent the LTCs and SCs operating limits, respectively. Observe that, since the demand varies over the day, the LTCs and SCs would switch frequently in order to maintain the voltages within limits; however, this will negatively impact the life, operation, and maintenance costs of the LTCs and SCs in the long term. Therefore, limits on the number of switching operations per day (5 times) and limits on maximum step changes over consecutive hours (± 3 steps) for LTCs and SCs are imposed in the DOPF model during its solution process. Depending on the purpose and model of controllable smart loads represented by (2c), the LDC can send signals such as peak demand constraints or temperature setpoints to these loads.

In order to study the effect of PS+ controllable loads, the average load model developed using NN for these loads are integrated into the DOPF model. The DOPF model determines the optimal decisions from the LDC's perspective, such as the LTC tap positions and number of capacitor blocks switched on, as well as the optimal ON/OFF signals to PCTs of ACs to reduce the peak load at the feeder level under the PS+ program.

Hence, two different DOPF models are proposed, the first objective function J_1 seeks to minimize the energy losses over the day, given as follows:

$$\begin{aligned} &\min\; J_1 = E_{loss} = \\ &\sum_h \sum_n \sum_p Re(V_{p,s_n,h} I_{p,s_n,h}^* - V_{p,r_n,h} I_{p,r_n,h}^*) \end{aligned} \tag{5}$$

with the following constraints to limit the feeder peak load:

$$\max(P_{feeder_{p,h}}) \leq P_{lim} \qquad \forall\, p, h \tag{6a}$$

$$\sum_h \mu_{p,n,h} \leq T_{p,n}^{max} \qquad \forall\, p, n \tag{6b}$$

$$P_{feeder_{p,h}} = Re(V_{p,s_f,h} I_{lf,p,h}^*) \qquad \forall\, p, h \tag{6c}$$

where (6a) is the substation feeder active power limit, and (6b) limits the maximum hours of PCT operation. However, the hard constraint (6a) may yield infeasible results, as it forces the control variables to reduce the demand below P_{lim}, which might not be feasible depending on the available controllable loads. Hence, a second objective function J_2 is defined that seeks to keep the load profile close to a target demand P_{cons} as follows:

$$\min \quad J_2 = E_{loss} + \beta S \tag{7a}$$

$$\text{s.t.} \quad \sum_h \mu_{p,n,h} \leq T_{p,n}^{max} \qquad \forall\, p, n \tag{7b}$$

$$S = \sum_h \sum_p |P_{feeder_{p,h}} - P_{cons}| \tag{7c}$$

As shown in Fig. 6, when the feeder power exceeds P_{cons}, PS+ loads will be activated by forcing $\mu_{p,n,h} = 1$, thus reducing the peak demand during the hours when $P_{feeder} > P_{cons}$; otherwise, $\mu_{p,n,h} = 0$ when $P_{feeder} < P_{cons}$. Hence, including S as defined in (7c) to the objective function (7a) reduces the

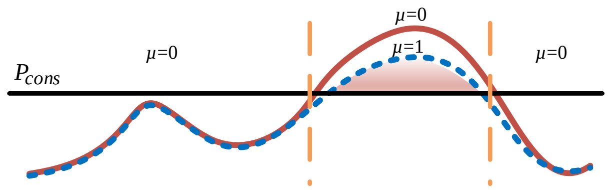

Fig. 6. ON/OFF decision making during peak load based on the value of P_{cons}.

load profile during the peak hours, forcing the load to be closer to the target demand P_{cons}.

The unbalanced DOPF model is solved using a recursive GA-based approach, which runs the Distribution Load Flow (DLF) of the feeder with unbalanced three-phase loads, using OpenDSS [33]. PS+ controllable loads are modeled using an NN, as previously discussed, and are integrated into OpenDSS as a controllable power demand variable defined by (1), as a function of the binary decision variable $\mu_{p,n,h}$, whereas the rest of the loads are represented as polynomial ZIP loads.

In order to make the DOPF model suitable for real-time application, the DLF model is treated as a stand-alone executable program that can be used on different platforms (i.e., Windows, Linux, and Mac). To reduce the computational costs of the DOPF model, and speed up the algorithm, a previously developed decentralized approach, referred to as the SGCM system [19], is used. The SGCM system is a software system designed for smart grid applications, which provides reliable, secure, and fast two-way communication amongst computing nodes of utility servers and smart sensors/controllers, which are able to run stand-alone executable files. Thus, in the GA procedure, the individuals are distributed from the master-node among different worker-nodes of the SGCM system, and the results obtained in each worker-node are then combined in the master-node for ranking, based on the objective function value. If the GA solution does not change for a number of generations, the processing time reaches the generation time limit, or number of generations reaches the maximum number of generations, the GA is considered to have converged, which means that the solution has been obtained; otherwise, the individuals are updated by cross-over and mutation operators of the GA, for the next iteration. The solution of the DOPF model is the 24-hour optimal LTC tap positions, number of capacitor blocks switched on, and ON/OFF PS+ signals for controllable smart loads.

IV. Results and Discussions

The aforementioned unbalanced DOPF with an NN model of PS+ loads was applied to the optimal dispatch of a practical unbalanced distribution feeder with 41 nodes, shown in Fig. 7 [34]. The system has three three-phase transformers equipped with 32-step LTCs, one single-phase transformer, and 10% of the loads are assumed to be PS+ controllable loads, while the rest of the loads are modeled as ZIP loads with a mix of 60% Z, 30% I, and 10% P components. More

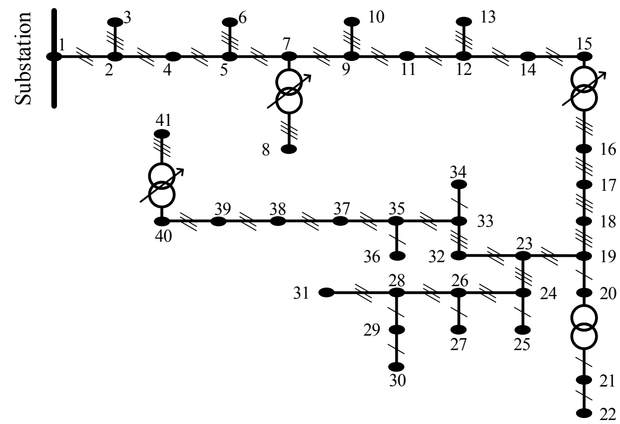

Fig. 7. Practical distribution test feeder [34].

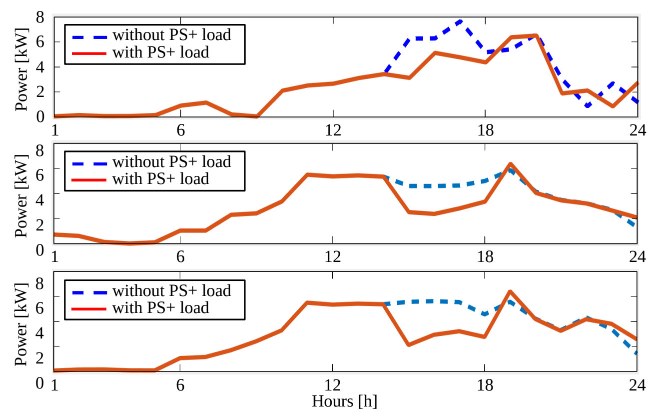

Fig. 8. Effect of PS+ signal on load profiles for hours 14:00 to 18:00 on three different days in July, 2013.

information about the system and simulation configuration is available in [19]. In order to consider realistic load variations, a load scaling factor is used taking into account the fluctuations in active and reactive power over the day. Furthermore, controllable PS+ load profiles, which vary from hour to hour, are determined from the NN model. Hence, the system load varies over the optimization horizon.

A. Case 1: J_1 Objective with Nodal and Phase-Wise Application of PS+ Signals

PS+ loads are currently activated in Ontario, Canada, during the summer weekdays (i.e., June to September) for a maximum of 4 hours at anytime, during a day. In this study, without loss of generality, the maximum ON hours are increased to 13, within a fixed window from hours 7:00 to 20:00 on weekdays to allow studying the effect of more flexible controllable loads. According to the PS+ rules, PCTs can be activated on average five times per year, up to a maximum of 40 hours, excluding emergencies such as a blackout during summer; however, in this research, it is assumed that these loads can be activated for longer periods of time.

Figure 8 shows the effect of PS+ signal on the feeder load

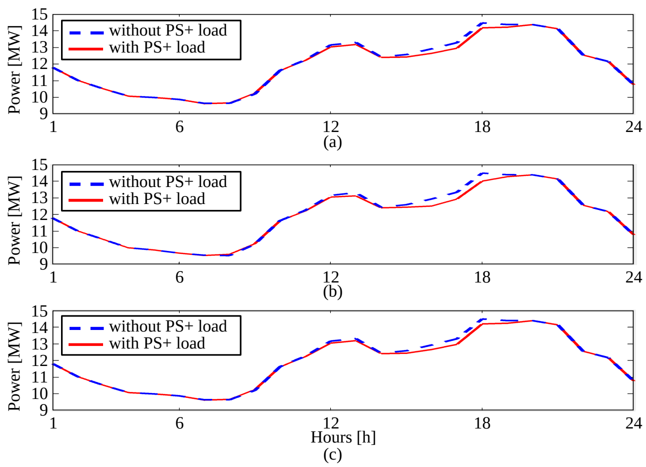

Fig. 9. Load profiles at the feeder level for $T_{p,n}^{max}$ of (a) 4, (b) 10, and (c) 13 hours, from hours 7:00 to 20:00.

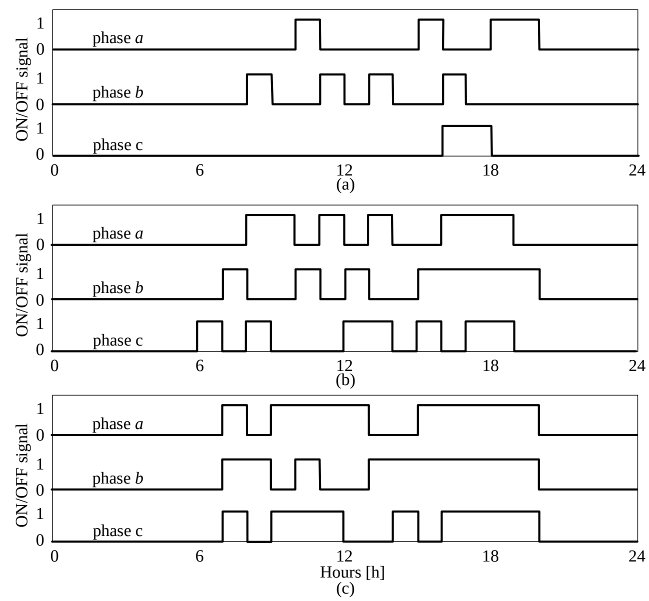

Fig. 10. Smart load activation signals μ at node 8 for $T_{p,n}^{max}$ of (a) 4, (b) 10, and (c) 13 hours, from hours 7:00 to 20:00.

profile for three different days. Observe the impact on load profiles when PS+ loads are activated between hours 14:00 and 18:00, showing a reduction in demand during these times, but it results in moving the peak to later hours in some cases, which can be attributed to HVAC operation.

For the DOPF model (5)-(6c), based on different experiments, P_{lim} was set to 14.5 MW, which is the minimum possible value that can be reached and solutions with P_{lim} less than 14.5 MW were infeasible. For different maximum hours of PCT operation from hours 4 to 13, simulations were performed, with each phase of each node receiving unique μ signals, i.e., PS+ loads located in different nodes and phases have different μ values. The results obtained show that by increasing $T_{p,n}^{max}$, the energy usage gradually decreasing, as shown in Fig. 9; for $T_{p,n}^{max}$ of 4, 10, and 13 hours, the energy savings are 1470.4, 1877.6, and 2048.9 kWh, respectively. Figure 10 depicts the μ signals sent to node 8 for each phase for $T_{p,n}^{max}$ of 4, 10, and 13 hours of PCT control; this node houses 70 PS+ customers in phase a, 60 in phase b, and 80 in phase c. Although the energy consumption decreases by increasing $T_{p,n}^{max}$, the peak load reduction for different hours does not change considerably.

It is worth mentioning that the PCT signals do not work effectively during extreme temperature conditions. Thus, in low temperatures, when the ACs are normally OFF, the PCT signals have no impact on their energy usage. Similarly, during high temperatures, ACs are normally ON, and increasing the setpoint by 2°C does not turn the ACs off, not affecting the energy usage of the system. Hence, this program is not effective during extreme hot summer-days, unless an AC cycling approach is used [35], [36].

B. Case 2: J_2 Objective with Uniform Application of PS+ Signals

Since J_1 seeks to minimize E_{loss}, increasing $T_{p,n}^{max}$ may reduce the energy usage, and consequently reduce E_{loss}; but, peak load reduction may not take place, as shown in Fig. 9. Hence, the J_2 objective in (7a)-(7c) can be used to reduce both E_{loss} and the peak load. In this case, it is assumed that the same PCT signal is sent to all PS+ controllable loads. The effect of β in (7c) for T^{max} = 4 h and P_{cons} = 11.5 MW is studied. Since in J_2 the target is to keep the peak load close to P_{cons}, the value of P_{cons} is chosen to be less than P_{lim} in order to effectively reduce the peak. Table I shows the effect of different values of β with uniform application of PS+ signals; it is noted that when β = 0, the peak load reduction achieved is 99.9 kW. Furthermore, when β is varied over a wide range, the peak load reduction remains more or less at the same level (95 to 100 kW). Thus, the peak load reduction is almost independent of β. However, note that increasing β increases the saving in energy usage from 1.62 to 2.38 MWh.

The impact of hours of PS+ operation on the energy usage and the peak loads are presented in Table II for β = 1 and P_{cons} = 11.5 MW, for T^{max} = 4-13 hours of PCT operation. Observe that for T^{max} = 4-9 hours of PCT operation, the peak loads are not considerably reduced, while for T^{max} = 10-13 hours, peak loads are efficiently decreased (up to 3.5 times further decrease in peak load). By increasing the maximum hours of ON signals, the DOPF model tends to activate the PCT for more hours, and hence the chance of reducing the peak load increases. The reduction of energy usage with T^{max} = 4 h is 1.58 MWh, while this reduction is 3.03 MWh with T^{max} = 13 h. Hence, offering further incentives to customers to opt for a higher value of T^{max} should be considered.

C. Case 3: J_2 Objective with Nodal and Phase-Wise Application of PS+ Signals

In this case, the effect of sending different PCT signals to the PS+ controllable loads in each phase and node of the distribution system, instead of sending the same PCT signal to all controllable loads, is studied. The results are presented in Table III. Comparing this table to Table I shows that different

TABLE I
J_2 OBJECTIVE WITH UNIFORM APPLICATION OF PS+ SIGNALS WITH T^{max} = 4 HOUR AND P_{cons} = 11.5 MW

β	Energy usage [MWh]			Peak load [kW]		
	Without PS+ signals	With PS+ signals	Difference	Without PS+ signals	With PS+ signals	Difference
0	287.61	285.99	1.62	14,575.5	14,475.6	99.9
0.01	287.61	285.99	1.62	14,597.7	14,501.7	96.0
0.02	287.81	286.16	1.65	14,549.5	14,449.7	99.8
0.1	288.09	286.37	1.71	14,597.8	14,501.6	96.2
0.15	287.76	286.01	1.75	14,542.8	14,446.5	96.3
1	287.27	285.09	2.18	14,476.7	14,378.2	98.5
2	287.79	285.40	2.38	14,540.0	14,445.4	94.6

TABLE II
J_2 OBJECTIVE WITH UNIFORM APPLICATION OF PS+ SIGNALS WITH β = 1 AND P_{cons} = 11.5 MW

PS+ ON signal hours	Energy usage [MWh]			Peak load [kW]		
	Without PS+ signals	With PS+ signals	Difference	Without PS+ signals	With PS+ signals	Difference
4	286.67	285.09	1.58	14,476.7	14,378.2	98.5
5	287.36	284.81	2.55	14,506.7	14,411.0	95.7
6	288.13	285.64	2.49	14,509.7	14,412.3	97.4
7	286.31	283.55	2.76	14,440.6	14,342.7	97.9
8	287.19	284.52	2.67	14,476.7	14,378.2	98.5
9	288.07	285.66	2.42	14,448.3	14,342.8	105.5
10	288.29	286.15	2.15	14,476.7	14,137.4	339.3
11	287.94	284.61	3.34	14,509.7	14,171.1	338.6
12	286.92	283.55	3.37	14,476.7	14,137.4	339.3
13	287.08	284.05	3.03	14,509.7	14,171.1	338.6

TABLE III
J_2 OBJECTIVE WITH NODAL AND PHASE-WISE APPLICATION OF PS+ SIGNALS WITH T^{max} = 4 HOUR AND P_{cons} = 11.5 MW

β	Energy usage [MWh]			Peak load [kW]		
	Without PS+ signals	With PS+ signals	Difference	Without PS+ signals	With PS+ signals	Difference
0	287.06	286.09	0.97	14,509.7	14,404.8	104.9
0.01	287.34	286.36	0.97	14,509.7	14,374.6	135.1
0.02	287.40	286.25	1.15	14,476.7	14,340.0	136.7
0.1	288.51	287.34	1.17	14,473.6	14,326.6	147.0
0.15	288.66	287.45	1.20	14,509.7	14,352.6	157.1
1	289.20	287.99	1.21	14,509.7	14,309.5	200.2
2	289.12	287.85	1.28	14,502.8	14,301.3	201.5

signals yield more reduction in peak load, but the energy usage increases. In this case, loads with higher peak load in each phase are activated, and hence the overall peak load is reduced more effectively than in the case of a uniform PS+ signal (Case 2); for instance, with β = 2 the peak load reduction in Case 3 is almost double that in Case 2. However, different signals reduces the savings in energy; for example, for β = 2, the saving in the energy usage is 2.38 MWh in Case 2, whereas this value is 1.28 MWh in the present case. Hence, based on the need of the system and also the DR program, LDCs need to decide what method is more suitable for them.

D. Discussion

The values of energy usage and peak load with different β and maximum PS+ signal hours in the case of no PS+ signals should ideally be the same. However, the variations observed are because of the GA-based solution technique adopted, which result on slightly different optimal decisions in every execution, and hence yield minor variations in the values of energy usage and peak load.

The effect of the PS+ program on the distribution feeder operation over a day is presented in Table IV. The best scenario in terms of energy loss from each of the PS+ cases previously discussed are used for comparison purposes. Note that all cases lead to a reduction in energy losses, energy usage, and energy costs for the system with respect to the Base Case with no PS+ signals. Observe also that Case 2 presents the best performance, with a 5.3% reduction in energy losses, 3.4% reduction in energy usage, and 2.8% reduction in energy costs. This shows that using the VVC objective of energy loss minimization in the DR program, effectively achieves both the VVC and DR objectives of energy loss, energy usage, and peak demand reductions. Note that this is achieved with a relatively low penetration of PS+ loads (10%), and thus increasing the number of controllable loads in the system would likely lead to further improvements in system operation.

The computation time interval of the DOPF model is one hour in this study, since the focus is on the feeder operations and thus a shorter time interval is not really necessary in this context. However, the proposed approach is able to achieve a minimum computation time of 15 minutes; hence, the

TABLE IV
COMPARISON OF CASE STUDIES

Cases	Energy losses [MWh]	Energy usage [MWh]	Energy costs [$]
Base Case (without PS+ signals)	7.21	293.51	26,835.44
Case 1 with T^{max} = 13 hours	6.85 (-5.0%)	288.17 (-1.8%)	26,421.96 (-1.5%)
Case 2 with β = 1 and T^{max} = 12 hours	6.83 (-5.3%)	283.55 (-3.4%)	26,078.78 (-2.8%)
Case 3 with β = 2 and T^{max} = 4 hours	6.99 (-3.1%)	287.85 (-1.9%)	26,376.21 (-1.7%)

DOPF could be solved every 15 minutes, if required for other applications. This reduction in computation time is possible because of the SGCM system used [19], which decentralizes the solution process. Therefore, if controllable loads need regular updates due to fast changes in their condition, shorter computing times may lead to more accurate load profiles and better solutions.

The studies presented in the paper demonstrate that modifications of some policies for the existing PS+ loads can effectively improve their impact on the reduction of peak demand and energy usage. For instance, it is shown in the paper that PCT activation for a longer period of time leads to higher reductions of peak loads in the system, which is of interest to LDCs. These proposed improvements to the existing controllable loads are also demonstrated to be necessary, since the simulation results show that the current limited time of operation of PS+ (4 hours) has insufficient impact on the reduction of peak load. Based on the presented results, it is shown that introducing some incentives for customers to opt for longer operation of PCTs would be beneficial for LDCs, with higher impact on the DR objective functions.

V. CONCLUSIONS

This paper proposed NN-based models of controllable loads, and studied the impact of Ontario's PS+ controllable loads on distribution feeders. Based on a distributed computing approach, an unbalanced DOPF model using a GA-based solution technique was proposed to determine the optimal setpoints for LTCs, SCs, and PS+ ON/OFF signals.

The studies carried out on a practical feeder demonstrated that different scenarios with single and multiple PCT ON/OFF signals for controllable loads could impact the load profiles, reduce peak loads, and decrease the energy usage. Based on the presented results, using a single ON/OFF signal for all controllable loads together with longer signal schedules could effectively reduce both peak loads and energy consumption of a distribution system at the feeder level, depending on the proportion of controllable loads in the system.

It is important to highlight that while DR programs can effectively reduce peak load and consequently energy usage, their impact on VVC objectives such as energy losses or energy drawn from the substation is also significant. Furthermore, appropriate incentives to motivate customers to opt for longer period of PCT operation, as shown in Case 2, can result in 3.5 times further decrease in peak load. Hence, LDCs can significantly gain from such programs by involving more customers for a longer period of time, since higher penetration of controllable loads would increase their impact on the DR objectives of reduction of peak load and energy usage, and on the VVC objective of energy loss minimization.

REFERENCES

[1] F. A. Rahiman, H. H. Zeineldin, V. Khadkikar, S. W. Kennedy, and V. R. Pandi, "Demand Response Mismatch (DRM): Concept, Impact Analysis, and Solution," *IEEE Trans. Smart Grid*, vol. 5, no. 4, pp. 1734 – 1743, July 2014.

[2] I. Roytelman and V. Ganesan, "Coordinated local and centralized control in distribution management systems," *IEEE Trans. Power Del.*, vol. 15, no. 2, pp. 718 – 724, Apr. 2000.

[3] L. Yu, D. Czarkowski, and F. de Leon, "Optimal Distributed Voltage Regulation for Secondary Networks With DGs," *IEEE Trans. Smart Grid*, vol. 3, no. 2, pp. 959 – 967, June 2012.

[4] M. C. Bozchalui, S. A. Hashmi, H. Hassen, C. A. Canizares, and K. Bhattacharya, "Optimal Operation of Residential Energy Hubs in Smart Grids," *IEEE Trans. Smart Grid*, vol. 3, no. 4, pp. 1755 – 1766, Dec. 2012.

[5] S. Paudyal, C. A. Canizares, and K. Bhattacharya, "Optimal Operation of Distribution Feeders in Smart Grids," *IEEE Trans. Ind. Electron.*, vol. 58, no. 10, pp. 4495 – 4503, Oct. 2011.

[6] I. Sharma, C. A. Cañizares, and K. Bhattacharya, "Residential microhub load model using neural network," in *2015 North American Power Symp. (NAPS)*, Oct. 2015, pp. 1 – 6.

[7] I. Lampropoulos, W. L. Kling, P. F. Ribeiro, and J. van den Berg, "History of demand side management and classification of demand response control schemes," in *Proc. 2013 IEEE Power Energy Society General Meeting (PES)*, July 2013, pp. 1 – 5.

[8] S. Wang and Z. Ma, "Supervisory and Optimal Control of Building HVAC Systems: A Review," *HVAC&R Research*, vol. 14, no. 1, pp. 3 – 32, Jan. 2008, [online]. Available: http://dx.doi.org/10.1080/10789669.2008.10390991.

[9] F. Zhao, J. Fan, and S. Mijanovic, "PI auto-tuning and performance assessment in HVAC systems," in *Proc. 2013 American Control Conf. (ACC)*, June 2013, pp. 1783 – 1788.

[10] Y. Sun, M. Elizondo, S. Lu, and J. C. Fuller, "The Impact of Uncertain Physical Parameters on HVAC Demand Response," *IEEE Trans. Smart Grid*, vol. 5, no. 2, pp. 916 – 923, Mar. 2014.

[11] M. Anderson, M. Buehner, P. Young, D. Hittle, C. Anderson, J. Tu, and D. Hodgson, "MIMO Robust Control for HVAC Systems," *IEEE Trans. Control Syst. Technol.*, vol. 16, no. 3, pp. 475 – 483, May 2008.

[12] "Peaksaver PLUS Frequently Asked Questions," *Hydro One*, [online]. Available: http://www.hydroone.com/MyHome/SaveEnergy/Pages/peaksaverPLUS_FAQs.aspx.

[13] S. Singla and S. Keshav, "Demand response through a temperature setpoint market in Ontario," in *Proc. 2012 IEEE 3rd Int. Conf. Smart Grid Communications (SmartGridComm)*, Nov. 2012, pp. 103 – 108.

[14] B.-K. Choi, H.-D. Chiang, Y. Li, H. Li, Y.-T. Chen, D.-H. Huang, and M. G. Lauby, "Measurement-based dynamic load models: derivation, comparison, and validation," *IEEE Trans. Power Syst.*, vol. 21, no. 3, pp. 1276 – 1283, Aug. 2006.

[15] S. Son, S. H. Lee, D.-H. Choi, K.-B. Song, J.-D. Park, Y.-H. Kwon, K. Hur, and J.-W. Park, "Improvement of Composite Load Modeling Based on Parameter Sensitivity and Dependency Analyses," *IEEE Trans. Power Syst.*, vol. 29, no. 1, pp. 242 – 250, Jan. 2014.

[16] D. Chen and R. R. Mohler, "Neural-network-based load modeling and its use in voltage stability analysis," *IEEE Trans. Control Syst. Technol.*, vol. 11, no. 4, pp. 460 – 470, July 2003.
[17] P. Regulski, D. S. Vilchis-Rodriguez, S. Djurović, and V. Terzija, "Estimation of Composite Load Model Parameters Using an Improved Particle Swarm Optimization Method," *IEEE Trans. Power Del.*, vol. 30, no. 2, pp. 553 – 560, Apr. 2015.
[18] P. Ju, E. Handschin, and D. Karlsson, "Nonlinear dynamic load modelling: model and parameter estimation," *IEEE Trans. Power Syst.*, vol. 11, no. 4, pp. 1689 – 1697, Nov. 1996.
[19] A. Mosaddegh, C. A. Cañizares, K. Bhattacharya, and H. Fan, "Distributed Computing Architecture for Optimal Control of Distribution Feeders with Smart Loads," *IEEE Trans. Smart Grid*, vol. PP, no. 99, pp. 1 – 10, Sept. 2016.
[20] E. Pouresmaeil, J. M. Gonzalez, C. A. Canizares, and K. Bhattacharya, "Development of a Smart Residential Load Simulator for Energy Management in Smart Grids," pp. 1 – 8, [online]. Available: https://uwaterloo.ca/power-energy-systems-group/downloads/smart-residential-load-simulator-srls.
[21] P. Palensky and D. Dietrich, "Demand Side Management: Demand Response, Intelligent Energy Systems, and Smart Loads," *IEEE Trans. Ind. Informat.*, vol. 7, no. 3, pp. 381 – 388, Aug. 2011.
[22] M. Dixon, "Autodaptive volt/VAr management system," in *Proc. 2001 Rural Electric Power Conf.*, May 2001, pp. D4/1 – D4/8.
[23] C.-h. Lien, Y.-w. Bai, and M.-b. Lin, "Remote-Controllable Power Outlet System for Home Power Management," *IEEE Trans. Consum. Electron.*, vol. 53, no. 4, pp. 1634 – 1641, Nov. 2007.
[24] M. A. A. Pedrasa, T. D. Spooner, and I. F. MacGill, "Coordinated Scheduling of Residential Distributed Energy Resources to Optimize Smart Home Energy Services," *IEEE Trans. Smart Grid*, vol. 1, no. 2, pp. 134 – 143, Sept. 2010.
[25] G. A. McNaughton and R. Saint, "Enterprise integration implications for home-area network technologies," in *Proc. 2010 Innovative Smart Grid Technologies (ISGT)*, Jan. 2010, pp. 1 – 5.
[26] Y. Liang, K. S. Tam, and R. Broadwater, "Load Calibration and Model Validation Methodologies for Power Distribution Systems," *IEEE Trans. Power Syst.*, vol. 25, no. 3, pp. 1393 – 1401, Aug. 2010.
[27] W. H. Kersting, *Distribution System Modeling and Analysis*, 3rd ed. Boca Raton: CRC Press, 2012.
[28] IEEE Task Force on Load Representation for Dynamic Performance, "Load representation for dynamic performance analysis [of power systems]," *IEEE Trans. Power Syst.*, vol. 8, no. 2, pp. 472 – 482, May 1993.
[29] A. Mosaddegh, C. A. Cañizares, and K. Bhattacharya, "Distributed computing approach to solve unbalanced three-phase DOPFs," in *Proc. 2015 IEEE Electrical Power and Energy Conf. (EPEC)*, Oct. 2015, pp. 408 – 413.
[30] A. Bokhari, A. Alkan, R. Dogan, M. Diaz-Aguilò, F. de Leòn, D. Czarkowski, Z. Zabar, L. Birenbaum, A. Noel, and R. E. Uosef, "Experimental Determination of the ZIP Coefficients for Modern Residential, Commercial, and Industrial Loads," *IEEE Trans. Power Del.*, vol. 29, no. 3, pp. 1372 – 1381, June 2014.
[31] A. Garces, "A Linear Three-Phase Load Flow for Power Distribution Systems," *IEEE Trans. Power Syst.*, vol. 31, no. 1, pp. 827 – 828, Jan. 2016.
[32] J. Y. Wen, L. Jiang, Q. H. Wu, and S. J. Cheng, "Power system load modeling by learning based on system measurements," *IEEE Trans. Power Del.*, vol. 18, no. 2, pp. 364 – 371, Apr. 2003.
[33] "Smart Grid Resource Center," *EPRI: Electric Power Research Institute*, [online]. Available: http://smartgrid.epri.com/SimulationTool.aspx.
[34] M. Graovac, X. Wang, and R. Iravani, "Integration of Storage in Electrical Distribution Systems and its Impact on the Depth of Penetration of DG," Clean Energy Technology Centre (CTEC), Tech. Rep. 2009-174, May 2008, [online]. Available: https://www.nrcan.gc.ca/sites/www.nrcan.gc.ca/files/canmetenergy/files/pubs/2009-174_RP-TEC_411-IMPACT_Graovac_Wang_Iravani_e.pdf.
[35] T. Facchinetti and M. L. Della Vedova, "Real-Time Modeling for Direct Load Control in Cyber-Physical Power Systems," *IEEE Trans. Ind. Informat.*, vol. 7, no. 4, pp. 689 – 698, Nov. 2011.
[36] W. Zhang, J. Lian, C. Y. Chang, and K. Kalsi, "Aggregated Modeling and Control of Air Conditioning Loads for Demand Response," *IEEE Trans. Power Syst.*, vol. 28, no. 4, pp. 4655 – 4664, Nov. 2013.

Abolfazl Mosaddegh (S'13) received the B.Sc. and M.Sc. degrees in electrical engineering from Iran University of Science and Technology, Tehran, Tehran, Iran in 2008 and 2011, respectively. He obtained his PhD in electrical and computer engineering from University of Waterloo, Waterloo, ON, Canada in 2016, and is currently working as a Research Associate at the same department. His research interests are in distributed computing approaches, distribution system modeling and analysis, and demand response programs in the context of smart grids.

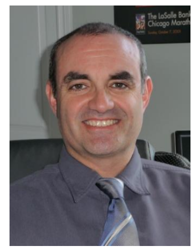

Claudio A. Cañizares (S'85-M'91-SM'00-F'07) received the Diploma degree in electrical engineering from Escuela Politecnica Nacional, Quito, Ecuador, and the M.S. and Ph.D. degrees in electrical engineering from the University of WisconsinMadison, Madison, WI, USA, in 1984, 1988, and 1991, respectively. He has held various academic and administrative at the University of Waterloo, ON, Canada, since 1993, where he is currently a Full Professor in the Department of Electrical and Computer Engineering and the Hydro One Endowed Chair. His research and consulting work concentrates on stability, operating, control, modeling, simulation, and computational issues in sustainable power and energy systems in the context of competitive markets, smart grids, and microgrids.

Dr. Cañizares was awarded the IEEE Canada Electric Power Medal in 2016, has received several IEEE Power and Energy Society (PES) Working Group Awards, and has held several leadership positions in PES Technical Committees and Subcommittees. He is a Fellow of the Royal Society of Canada and the Canadian Academy of Engineering, and is a Registered Professional Engineer in the province of Ontario.

Kankar Bhattacharya (M'95-SM'01-F'17) received the Ph.D. degree in electrical engineering from the Indian Institute of Technology, New Delhi, India, in 1993. He was with the Faculty of Indira Gandhi Institute of Development Research, Mumbai, India, from 1993 to 1998, and with the Department of Electric Power Engineering, Chalmers University of Technology, Gothenburg, Sweden, from 1998 to 2002. In 2003, he joined the Electrical and Computer Engineering Department, University of Waterloo, Waterloo, ON, Canada, where he is currently a Full Professor. His current research interests include power system economics and operational aspects. He is a Registered Professional Engineer in the province of Ontario.